UC Davis
UC Davis Previously Published Works

Title

A Salmonella Virulence Factor Activates the NOD1/NOD2 Signaling Pathway

Permalink

https://escholarship.org/uc/item/9w82p1c5

Journal

mBio, 2(6)

ISSN

2161-2129

Authors

Keestra, A Marijke
Winter, Maria G
Klein-Douwel, Daisy
et al.

Publication Date

2011-12-30

DOI

10.1128/mbio.00266-11

Peer reviewed

A *Salmonella* Virulence Factor Activates the NOD1/NOD2 Signaling Pathway

A. Marijke Keestra, Maria G. Winter, Daisy Klein-Douwel, Mariana N. Xavier, Sebastian E. Winter, Anita Kim, Renée M. Tsolis, and Andreas J. Bäumler

Department of Medical Microbiology and Immunology, School of Medicine, University of California, Davis, California, USA

ABSTRACT The invasion-associated type III secretion system (T3SS-1) of *Salmonella enterica* serotype Typhimurium (*S.* Typhimurium) activates the transcription factor NF-κB in tissue culture cells and induces inflammatory responses in animal models through unknown mechanisms. Here we show that bacterial delivery or ectopic expression of SipA, a T3SS-1-translocated protein, led to the activation of the NOD1/NOD2 signaling pathway and consequent RIP2-mediated induction of NF-κB-dependent inflammatory responses. SipA-mediated activation of NOD1/NOD2 signaling was independent of bacterial invasion *in vitro* but required an intact T3SS-1. In the mouse colitis model, SipA triggered mucosal inflammation in wild-type mice but not in NOD1/NOD2-deficient mice. These findings implicate SipA-driven activation of the NOD1/NOD2 signaling pathway as a mechanism by which the T3SS-1 induces inflammatory responses *in vitro* and *in vivo*.

IMPORTANCE *Salmonella enterica* serotype Typhimurium (*S.* Typhimurium) deploys a type III secretion system (T3SS-1) to induce intestinal inflammation and benefits from the ensuing host response, which enhances growth of the pathogen in the intestinal lumen. However, the mechanisms by which the T3SS-1 triggers inflammatory responses have not been resolved. Here we show that the T3SS-1 effector protein SipA induces NF-κB activation and intestinal inflammation by activating the NOD1/NOD2 signaling pathway. These data suggest that the T3SS-1 escalates innate responses through a SipA-mediated activation of pattern recognition receptors in the host cell cytosol.

Address correspondence to Andreas J. Bäumler, ajbaumler@ucdavis.edu.

The principal pathogenic strategy of *Salmonella enterica* serotype Typhimurium (*S.* Typhimurium) is to use its virulence factors to elicit acute intestinal inflammation (1). A by-product of this host response is the generation of a new respiratory electron acceptor, tetrathionate, which enables the pathogen to outgrow other microbes in the intestinal lumen (2), thereby enhancing its transmission (3). *S.* Typhimurium utilizes a type III secretion system (T3SS-1) encoded by *Salmonella* pathogenicity island 1 (SPI 1) to elicit intestinal inflammation in animal models (1, 4). The principal function of the T3SS-1 is to deliver proteins, termed effectors, into host cells (5, 6). Five T3SS-1 effectors, termed SipA, SopA, SopB, SopD, and SopE2, act in concert to trigger alterations in the actin cytoskeleton of host cells, thereby promoting epithelial invasion (7–11) and intestinal inflammation (12). *S.* Typhimurium induces activation of mitogen-activated protein (MAP) kinases, activation of nuclear factor kappa-light-chain-enhancer of activated B cells (NF-κB), and production of proinflammatory cytokines in cultured cell lines in a T3SS-1-dependent fashion (13), suggesting that cytosolic access by the T3SS-1 triggers host cell responses.

Several mechanisms through which cytosolic access by the T3SS-1 can induce inflammatory responses have been proposed. These mechanisms have in common that cytosolic access by the T3SS-1 is detected by host macrophages via cytosolic recognition of translocated bacterial proteins, resulting in caspase 1 activation

and consequent proteolytic activation of interleukin-1β (IL-1β) and IL-18, two proinflammatory cytokines (14–16). However, it is also clear that these mechanisms are not sufficient to explain important *in vitro* and *in vivo* observations, suggesting that additional pathways by which the T3SS-1 induces inflammatory responses remain to be discovered. Specifically, activation of caspase 1 cannot account for the T3SS-1-dependent activation of NF-κB observed *in vitro* (13). Furthermore, the invasion-associated T3SS-1 of *S.* Typhimurium elicits intestinal inflammation *in vivo* through a myeloid differentiation primary response protein 88 (MyD88)-independent mechanism (17). Caspase 1 activation does not explain the generation of these MyD88-independent proinflammatory responses, because MyD88 is required for signaling through receptors for IL-1β and IL-18 (18–20). Here we identify a new MyD88-independent mechanism by which the T3SS-1 induces host cell responses *in vitro* and demonstrate that this mechanism contributes to *S.* Typhimurium-induced intestinal inflammation *in vivo*.

RESULTS

NF-κB activation by the invasion-associated T3SS is invasion independent. The invasion-associated T3SS-1 of *S.* Typhimurium activates NF-κB in human epithelial cells (see Fig. S1A in the supplemental material) (13, 21). To analyze whether this process is invasion dependent, we used human epithelial cells transfected
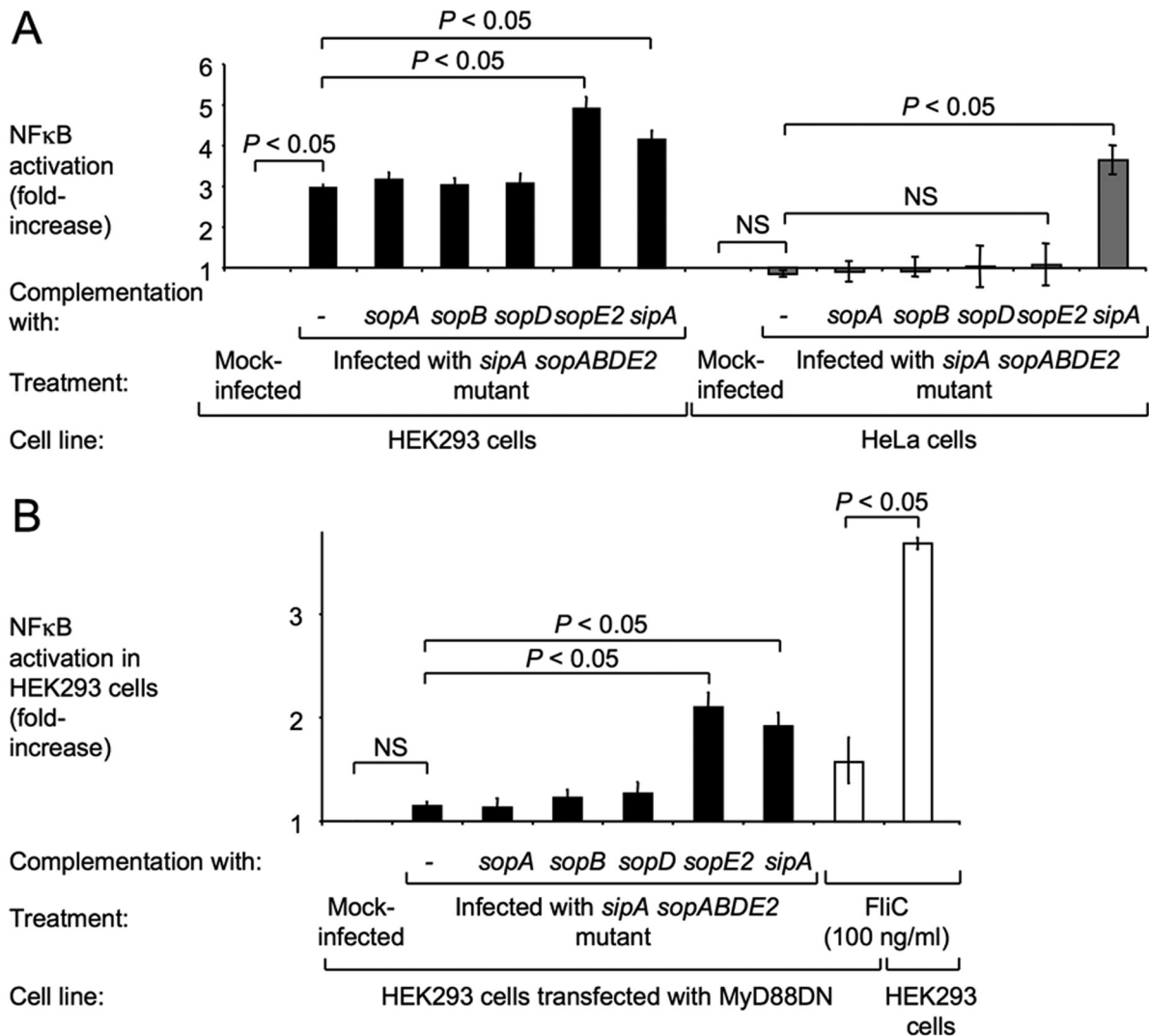
FIG 1 SipA-mediated activation of NF-κB in HeLa and HEK293 cells is MyD88 independent. (A) HeLa cells (gray bars) and HEK293 cells (black bars) transfected with an NF-κB luciferase reporter construct were infected with the *S.* Typhimurium *sipA sopABDE2* mutant complemented with genes encoding the indicated effector proteins. (B) HEK293 cells were transfected with MyD88DN and infected with the *S.* Typhimurium *sipA sopABDE2* mutant and complemented derivatives. Data represent the NF-κB luciferase activity as fold increase over the uninfected controls. Values are the means from at least 3 independent experiments ± standard errors. Brackets indicate the statistical significance of differences. NS, not significant.

with an NF-κB luciferase reporter construct. A T3SS-1-deficient *S.* Typhimurium mutant (*invA* mutant) neither activated NF-κB (Fig. 1A) nor invaded epithelial HeLa cells (Fig. S1B). Introduction of the *Yersinia pseudotuberculosis* invasin protein (22) increased invasiveness of the T3SS-1-deficient *S.* Typhimurium mutant ($P < 0.05$) but did not restore NF-κB activation. Similar results were obtained with human embryonic kidney 293 (HEK293) cells, although inactivation of the invasion-associated T3SS resulted only in a partial inhibition of NF-κB activation in this cell line (Fig. S1C and S1D).

The T3SS-1 effectors SipA, SopA, SopB, SopD, and SopE2 act in concert to promote invasion of epithelial cells (10). An *S.* Typhimurium mutant lacking these five effector proteins (*sipA sopABDE2* mutant) was deficient for invasion ($P < 0.05$) and NF-κB activation ($P < 0.05$) (see Fig. S1 in the supplemental material). Introduction of the *Y. pseudotuberculosis* invasin protein into the

sipA sopABDE2 mutant restored invasiveness ($P < 0.05$) but not NF-κB activation. These data suggested that NF-κB activation required delivery of T3SS-1 effector proteins but not bacterial invasion.

SipA is a key mediator of NF-κB activation *in vitro*. To determine whether host cells can sense delivery of specific effectors, we complemented the *S.* Typhimurium *sipA sopABDE2* mutant with plasmids encoding SipA, SopA, SopB, SopD, or SopE2 (10) and monitored NF-κB activation (Fig. 1). Only a plasmid encoding SipA complemented the *sipA sopABDE2* mutant for NF-κB activation in epithelial HeLa cells ($P < 0.05$) (Fig. 1A). Endogenous TLR5 expression renders HEK293 cells responsive to stimulation with flagellin (23, 24), which might explain why we observed NF-κB activation in response to infection with the *sipA sopABDE2* mutant or to stimulation with purified *S.* Typhimurium flagellin (FliC) ($P < 0.05$) in this cell line (Fig. 1A and 1B). Consistent with
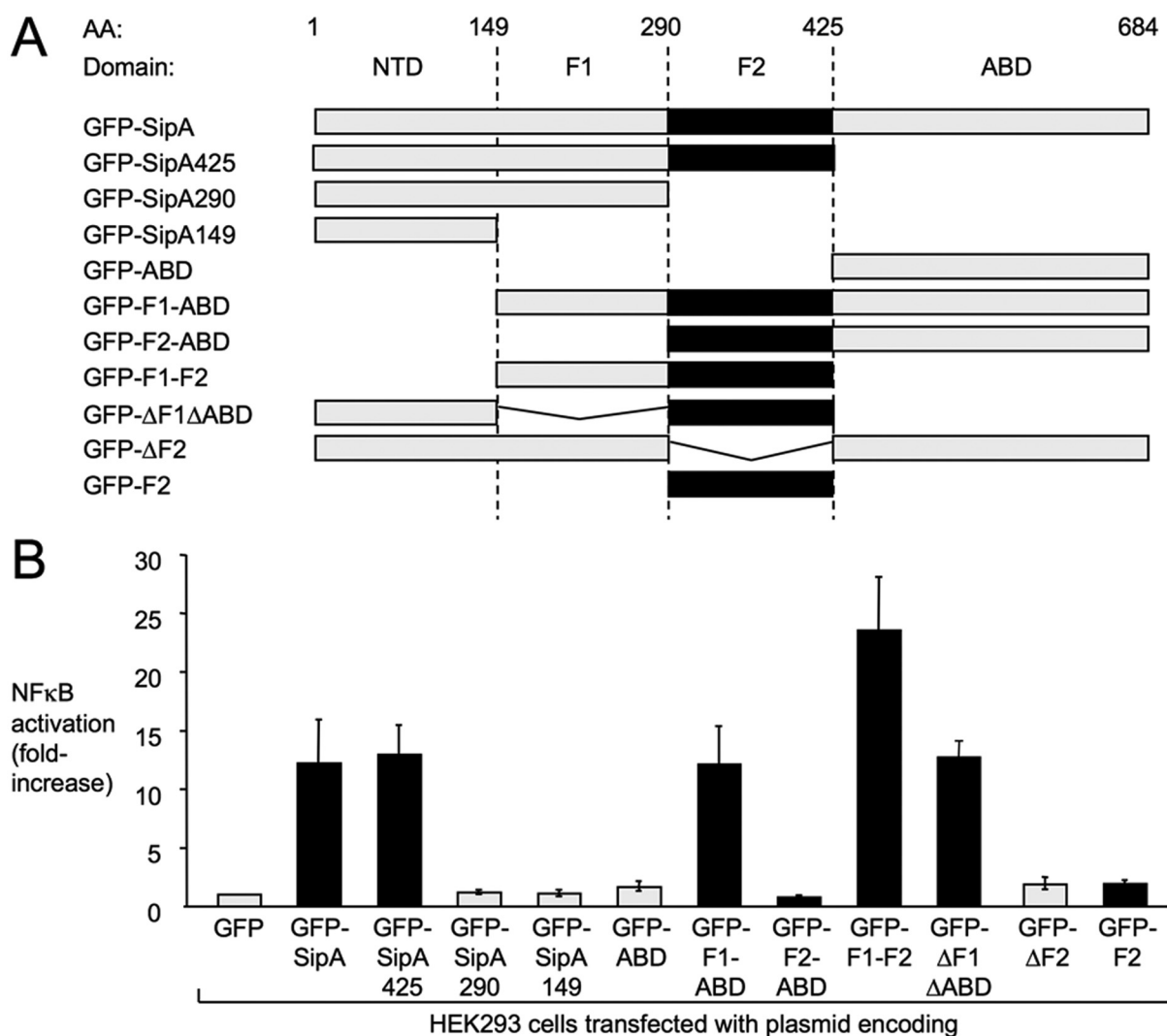
FIG 2 The F2 domain of SipA is necessary but not sufficient for NF-κB activation. (A) Schematic representation of the SipA domain structure (top). The composition of GFP-SipA fusion proteins is indicated below. (B) HEK293 cells were cotransfected with an NF-κB luciferase reporter construct and the indicated GFP-SipA fusion proteins. At 48 hours after transfection, cells were lysed to measure luciferase activity. Data represent the means ± standard errors of at least three independent experiments.

this idea, transfection of HEK293 cells with a plasmid encoding a dominant-negative form of the TLR5 adaptor protein MyD88 (MyD88DN) abrogated NF-κB activation induced by the *sipA sopABDE2* mutant or purified flagellin (Fig. 1B). Complementation of the *sipA sopABDE2* mutant with plasmids encoding SipA or SopE2 induced NF-κB activation in HEK293 cells transfected with MyD88DN ($P < 0.05$) (Fig. 1B). Collectively, these data suggested that bacterial delivery of SipA activates NF-κB through a MyD88-independent mechanism.

To determine whether SipA is sufficient for NF-κB activation, a green fluorescent protein (GFP)-SipA fusion protein was expressed ectopically in HEK293 cells transfected with an NF-κB luciferase reporter construct (Fig. 2). Ectopic expression of GFP-SipA, but not ectopic expression of GFP, resulted in NF-κB activation ($P < 0.05$). These data suggested that cytosolic localization of SipA in the absence of other bacterial molecules was sufficient for inducing NF-κB activation in host cells.

The SipA protein contains an N-terminal domain required for T3SS-1 translocation (NTD), a C-terminal actin-binding domain (ABD), and two central domains mediating SipA focus formation (F1) and SipA-SipA interaction (F2) (25). GFP-SipA fusion proteins lacking one or several of these domains were constructed to investigate which domain(s) is required for NF-κB activation (Fig. 2A). Ectopic expression of these fusion proteins in HEK293 cells suggested that the F2 domain, which is not required for host cell invasion (25), was necessary but not sufficient for NF-κB activation ($P < 0.05$) (Fig. 2B; see also Fig. S2 in the supplemental material). In contrast, the ABD, which is required to support *S.* Typhimurium host cell invasion (25), was not necessary for NF-κB activation.

To determine whether the F2 domain was necessary for NF-κB activation upon bacterial delivery of SipA, we complemented the *sipA sopABDE2* mutant with plasmids carrying truncated *sipA* genes encoding the first 425 amino acids (aa) (*sipA'*1-425), the
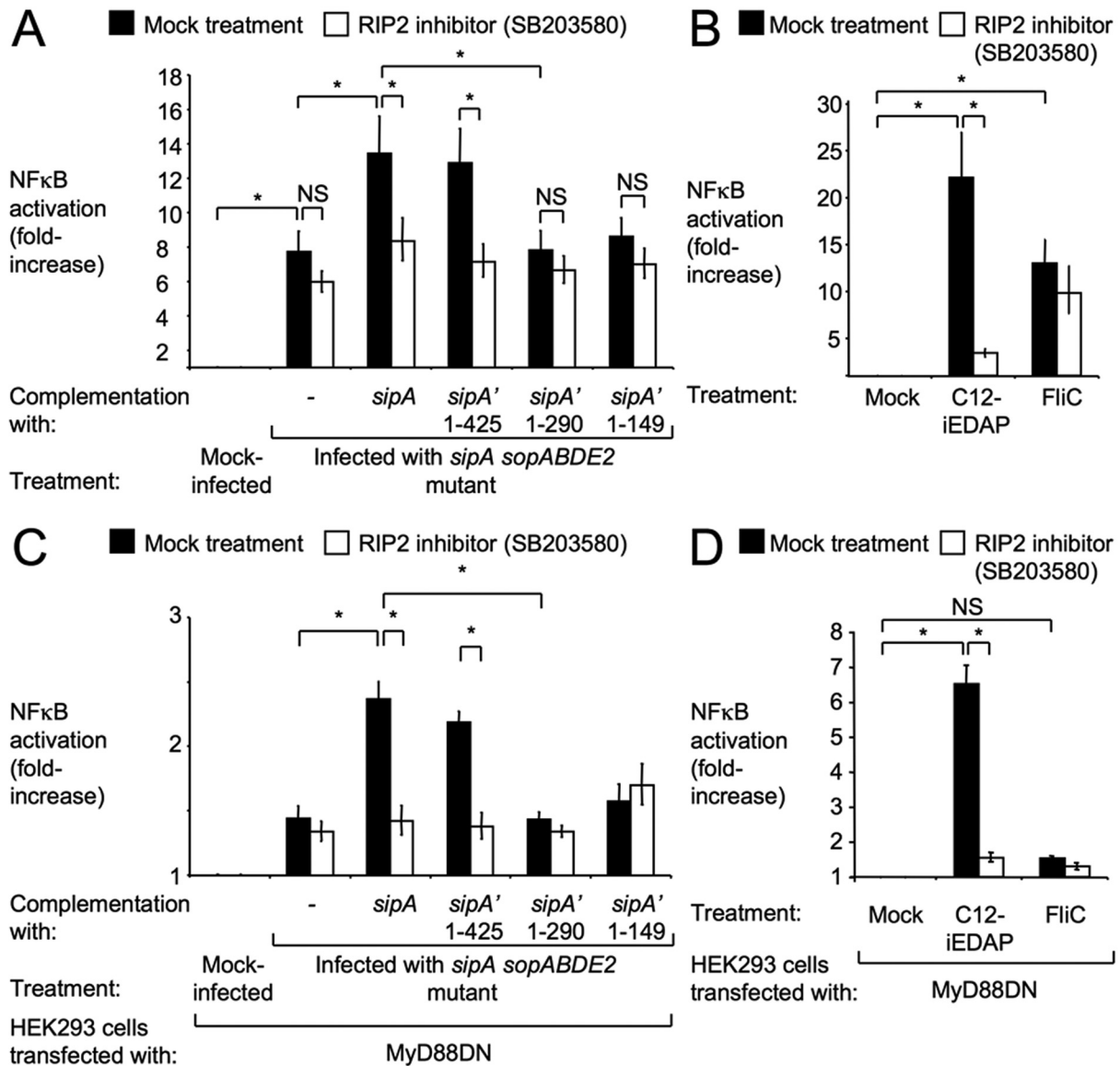
FIG 3 The RIP2 inhibitor SB203580 inhibits SipA-mediated NF-κB activation. HEK293 cells were transfected with an NF-κB luciferase reporter construct (A and B) and MyD88DN (C and D). Thirty minutes before infection of the cells with the indicated *S.* Typhimurium strains, the cells were pretreated with dimethyl sulfoxide (black bars) or with 10 μM SB203580 (white bars). After 5 h, the cells were lysed and luciferase activity was measured. Data represent the means ± standard errors of at least three independent experiments. Brackets indicate the statistically significant differences. *, $P < 0.05$. NS, not significant.

first 290 amino acids (*sipA*'1-290), or the first 149 amino acids (*sipA*'1-149) of SipA. Complementation of the *sipA sopABDE2* mutant with genes encoding full-length SipA or a truncated SipA lacking the ABD (*sipA*'1-425) resulted in NF-κB activation through a MyD88-independent mechanism (Fig. 3). In contrast, NF-κB activation was not observed with proteins lacking the F2 domain, which were encoded by *sipA*'1-290 and *sipA*'1-149. In summary, the F2 domain was necessary for NF-κB activation regardless of whether SipA was delivered by bacteria or expressed ectopically.

SipA-mediated NF-κB activation requires RIP2 *in vitro.* One MyD88-independent mechanism contributing to intestinal inflammation during *S.* Typhimurium infection is the activation of nucleotide-binding and oligomerization domain 1 (NOD1) and

NOD2, two intracellular sensors of bacterial cell wall fragments (26, 27). NOD1 and NOD2 interact with protein kinase receptor-interacting protein 2 (RIP2) to mediate NF-κB activation (28, 29). Stimulation of HEK293 cells with the NOD1 ligand C12-iE-DAP resulted in NF-κB activation ($P < 0.05$), which was MyD88 independent and could be inhibited with SB203580 (Fig. 3B and 3D), a pyridinyl imidazole inhibitor of RIP2 activity (30). NF-κB activation induced by bacterial delivery of SipA was abrogated when cells were treated with the RIP2 inhibitor SB203580 (Fig. 3A and 3C). These data suggested that SipA-mediated NF-κB activation required RIP2.

SipA-mediated NF-κB activation requires both NOD1 and NOD2 *in vitro.* We next investigated whether NOD1 or NOD2 was required for SipA-dependent NF-κB activation (Fig. 4).
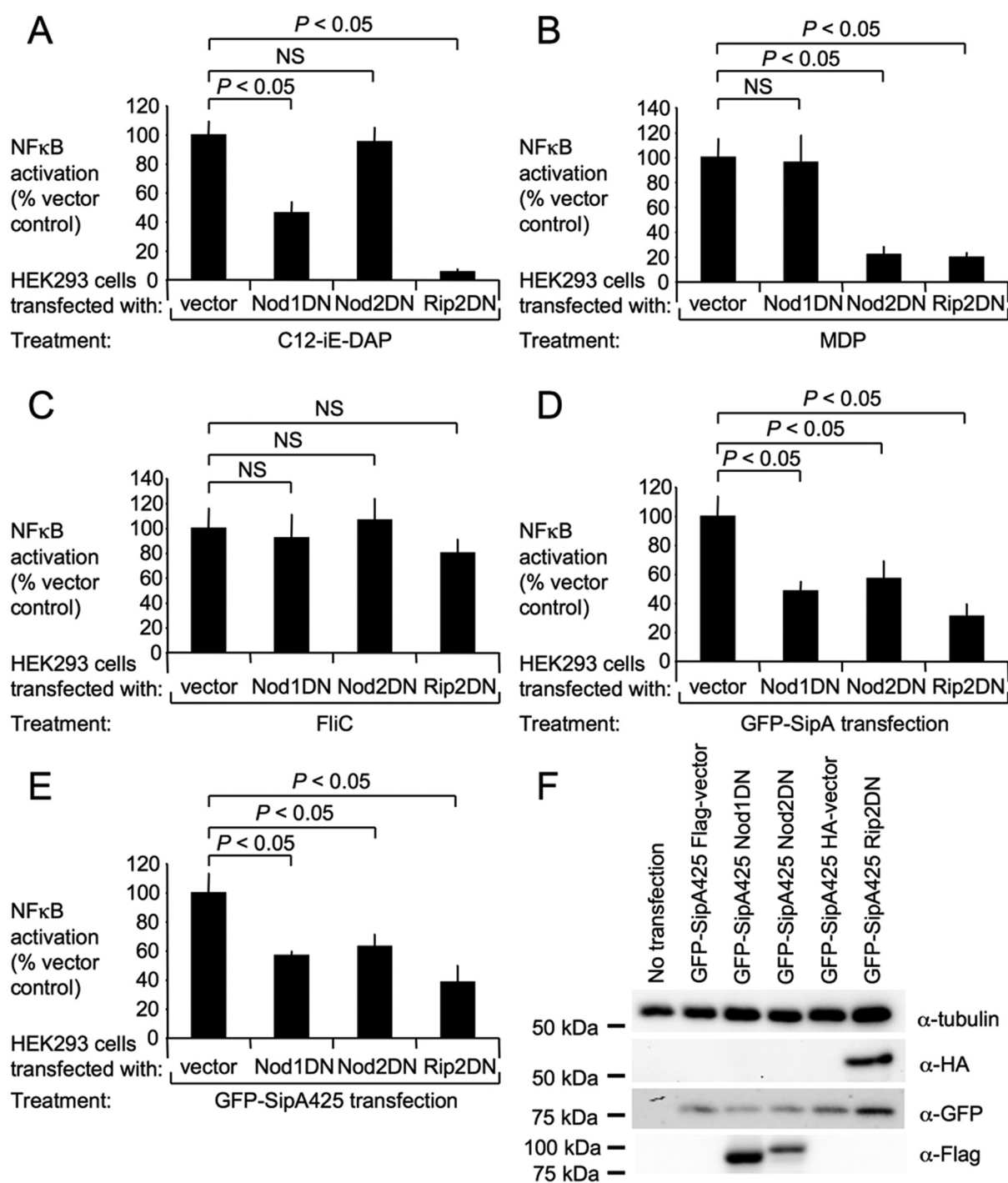
FIG 4 SipA-mediated NF-κB activation requires both NOD1 and NOD2 *in vitro*. (A to C) HEK293 cells were transfected with the NF-κB luciferase reporter construct and hNOD1DN, hNOD2DN, hRIP2DN, or vector only and stimulated with 1 μg/ml C12-iE-DAP (NOD1 ligand) (A), 10 μg/ml MDP (NOD2 ligand) (B), and 100 ng/ml purified flagellin (C). (D and E) HEK293 cells were cotransfected with the NF-κB luciferase reporter construct and GFP-SipA (D) or GFP-SipA425 (E) and hNOD1DN, hNOD2DN, hRIP2DN, or vector only. Data are expressed as percent NF-κB inhibition, where 100% was set to be the response in the cells transfected with vector only. Values represent the means ± standard errors of at least three independent experiments. Brackets indicate the statistical differences. NS, not significant. (F) Western blot analysis of HEK293 cells expressing GFP-tagged SipA425 and Flag-tagged hNOD1DN, Flag-tagged hNOD2DN, HA-tagged hRIP2DN, or vector only. Cotransfection did not influence the expression of GFP-SipA425.

Transfection of HEK293 cells with plasmids encoding a dominant-negative NOD1 protein (Nod1DN) or a dominant-negative RIP2 protein (Rip2DN) inhibited NF-κB activation elic-ited by stimulation with the NOD1 ligand C12-iE-DAP (Fig. 4A). Similarly, transfection of HEK293 cells with dominant-negative NOD2 (Nod2DN) or Rip2DN inhibited NF-κB activation elicited
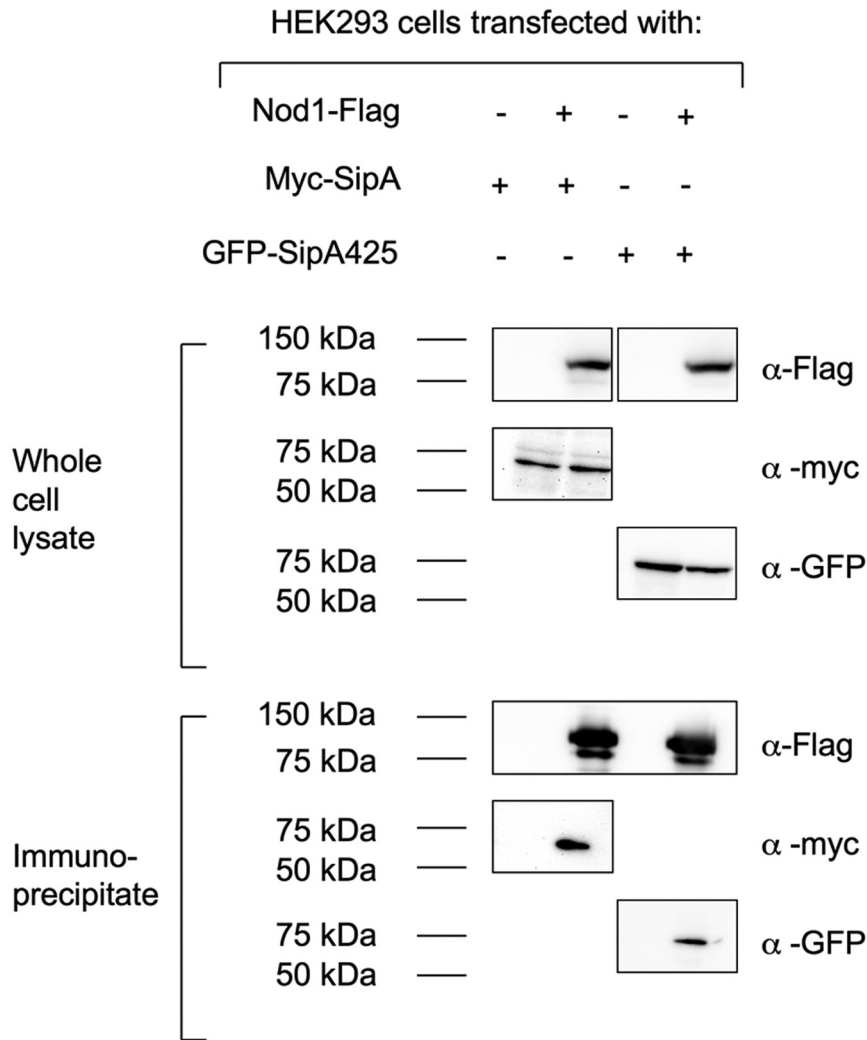
HEK293 cells transfected with:

FIG 5 Coimmunoprecipitation of NOD1 and SipA. At 48 hours after transfection of HEK293 cells with the indicated constructs, immunoprecipitation was performed using anti-Flag antibodies. Proteins were detected in whole-cell lysates and immunoprecipitates by Western blot analysis with anti-Flag antibody (α-Flag), anti-Myc antibody (α-myc), or anti-GFP antibody (α-GFP).

by stimulation with the NOD2 ligand muramyl dipeptide (MDP) (Fig. 4B). Dominant-negative forms of NOD1 (Nod1DN), NOD2 (Nod2DN), or RIP2 (Rip2DN) did not inhibit NF-κB activation in HEK293 cells stimulated with flagellin (FliC) (Fig. 4C). Importantly, transfection of HEK293 cells with dominant-negative forms of NOD1 (Nod1DN), NOD2 (Nod2DN), or RIP2 (Rip2DN) inhibited NF-κB activation elicited by ectopic expression of GFP-SipA or GFP-SipA425 ($P < 0.05$) (Fig. 4D and 4E). Cotransfection of the dominant-negative forms of NOD1, NOD2, or RIP2 with GFP-SipA425 did not markedly affect protein expression of SipA425 (Fig. 4F). Ectopic expression excluded the possibility that SipA-mediated NF-κB activation was due to contamination with endogenous bacterial ligands, such as MDP. Furthermore, both NOD1 and NOD2 contributed to NF-κB activation in response to ectopic expression of SipA (Fig. 4D), while responses to C12-iE-DAP required only NOD1 (Fig. 4A) and responses to MDP required only NOD2 (Fig. 4B). Collectively, these data suggested that SipA activated NOD1/NOD2 through a path-

way that was distinct from that observed with bacterial cell wall fragments.

To investigate interaction of SipA with NOD1, HEK293 cells were transfected with Flag-tagged NOD1 protein (NOD1-Flag) and either Myc-tagged SipA protein (Myc-SipA) or GFP-SipA425. After immunoprecipitation of Flag-NOD1 with anti-Flag antibody, SipA was detected in the immunoprecipitate (Fig. 5). Furthermore, colocalization of SipA and NOD1 was observed microscopically in some HEK293 cells transfected with NOD1-Flag and GFP-SipA (see Fig. S3 in the supplemental material). Collectively, these data suggested that SipA either interacts with NOD1 directly or is present in a protein complex that contains NOD1.

SipA does not trigger mucosal inflammation in NOD1/ NOD2-deficient mice. To test the biological significance of our observations, we determined the role of NOD1/NOD2 in SipA-mediated inflammation *in vivo* using the mouse colitis model of *S.* Typhimurium infection (4). The T3SS effectors SipA, SopA, SopB, SopD, and SopE2 act in concert to trigger intestinal inflam-
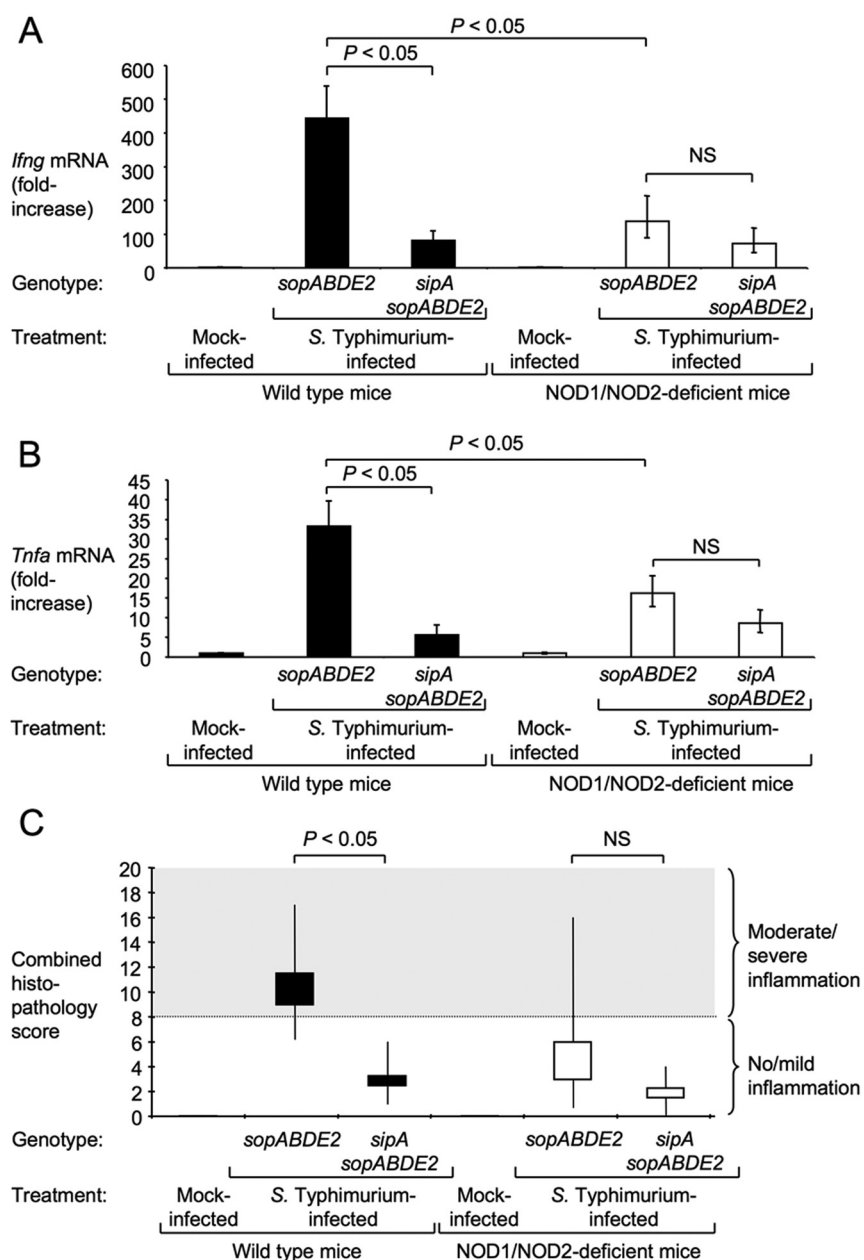
FIG 6 Inflammatory responses in the mouse colitis model. C57BL/6 mice (wild type, black bars) and NOD1/NOD2-deficient mice (white bars) were inoculated with the *S.* Typhimurium *sopABDE2* mutant, the *S.* Typhimurium *sipA sopABDE2* mutant, or sterile medium (mock infected), and cecal tissue was collected at 48 hours after infection. (A and B) Relative *Ifng* (A) and *Tnfa* (B) transcript levels in the cecal tissue were determined by quantitative real-time PCR. Bars represent the geometric means ± standard errors from eight different animals. Brackets indicate the statistical significance of differences. NS, not significant. (C) Histopathological analysis of the cecal mucosa. Boxes in whisker plots represent the second and third quartiles of combined histopathology scores, while lines indicate the first and fourth quartiles. Brackets indicate the statistical significance of differences. NS, not significant.

mation (12). To restrict our analysis to SipA-mediated mechanisms of inflammation, we compared an *S.* Typhimurium strain producing only SipA (*sopABDE2* mutant) with an isogenic SipA-deficient mutant (*sipA sopABDE2* mutant). Remarkably, the SipA-proficient *S.* Typhimurium strain (*sopABDE2* mutant) triggered mucosal inflammation in wild-type mice (C57BL/6) but not in the NOD1/NOD2-deficient mice 2 days after infection (Fig. 6; see also Fig. S4 in the supplemental material). NOD1/NOD2-deficient mice failed to induce SipA-dependent expression of *Ifng*,

the gene encoding gamma interferon (IFN-γ) (Fig. 6A), and *Tnfa*, the gene encoding tumor necrosis factor alpha (TNF-α) (Fig. 6B), in the cecal mucosa. Wild-type (C57BL/6) mice infected with the SipA-proficient *S.* Typhimurium strain (*sopABDE2* mutant) exhibited marked intestinal inflammation, which was absent in wild-type mice infected with the SipA-deficient mutant (*sipA sopABDE2* mutant) or in NOD1/NOD2-deficient mice (Fig. 6C; see also Fig. S4). In summary, a SipA-proficient *S.* Typhimurium

strain required NOD1/NOD2 for eliciting intestinal inflammation.

DISCUSSION

The translocation of multiple proteins by the T3SS-1 can mask the contribution of an individual pathway to inflammation *in vivo*. For example, previous studies show that *S.* Typhimurium can induce inflammation in mice deficient for MyD88, RIP2, or caspase 1 (31). However, when mice are infected with an *S.* Typhimurium strain translocating only the SopE protein (*sipA sopB sopE2 sseD* mutant), it becomes apparent that caspase 1 activation contributes to mucosal inflammation in the mouse colitis model (32). Similarly, here we show that a contribution of NOD1/NOD2 signaling to inflammation is apparent when mice are infected with an *S.* Typhimurium strain that translocates SipA but carries mutations in genes encoding other T3SS-1 effector proteins involved in eliciting intestinal inflammation.

SipA is a protein delivered into the host cell cytosol by the invasion-associated T3SS of *S.* Typhimurium (6). SipA contributes to invasion of epithelial cell lines by modulating actin assembly through its C-terminal ABD (6, 9–11, 25). The N-terminal 425 amino acids of SipA trigger neutrophil transepithelial migration *in vitro* (33–36). Finally, SipA contributes to intestinal inflammation *in vivo* (12, 37), but the underlying mechanism has remained unclear. Here we show that the proinflammatory effects of SipA required NOD1/NOD2 activity. Furthermore, *in vitro* experiments demonstrated that SipA was necessary and sufficient for NOD1/NOD2-dependent NF-κB activation, a process that did not require its ABD. These data suggested that cytosolic sensing of SipA by the pattern recognition receptors NOD1 and NOD2 served as a signal for cytosolic access by the invasion-associated T3SS-1 of *S.* Typhimurium, thereby escalating mucosal inflammatory responses. Consistent with this idea, SipA enhanced mucosal inflammation in the mouse colitis model in a NOD1/NOD2-dependent fashion.

MATERIALS AND METHODS

Bacterial strains, tissue culture cells, and culture conditions. *S.* Typhimurium strain IR715 (38), a fully virulent, nalidixic acid-resistant derivative of American Type Culture Collection (ATCC) isolate 14028, was used as a wild-type isolate. IR715 derivatives carrying mutations in *invA* (SPN449) (39); in *sopA, sopB, sopD*, and *sopE2* (ZA20) (12); and in *sipA, sopA, sopB, sopD*, and *sopE2* (ZA21) (12) have been described previously. Plasmids carrying the *sopD* gene (pMR15), the *sopE2* gene (pMR17), the *sopB* gene (pMR26), the *sopA* gene (pMR28), or the *sipA* gene (pMR29) from *S.* Typhimurium have been described previously (10). The *sipA425*, *sipA290*, and *sipA149* fragments of the *sipA* gene were amplified without the *sipA* promoter from pMR29 and cloned directionally behind the *lac* promoter of cloning vector pWSK29 (40) with BamHI and XbaI. Plasmid pRI203, encoding the *Yersinia pseudotuberculosis* invasin protein, has been described previously (22). Bacteria were grown aerobically at 37°C in Luria-Bertani (LB) broth supplemented with antibiotics. The HeLa 57A cell line stably transfected with an NF-κB luciferase reporter construct (41) was generously provided by R. T. Hay (the Wellcome Trust Centre for Gene Regulation and Expression, College of Life Sciences, University of Dundee, United Kingdom). The HEK293 cell line was purchased from ATCC. HeLa 57A cells and HEK293 cells were maintained in Dulbecco's modified Eagle's medium (DMEM) containing 10% fetal calf serum (FCS) at 37°C in a 5% CO₂ atmosphere.

Construction of expression plasmids. The *sipA* gene was PCR amplified from the chromosome of *S.* Typhimurium IR715, and the obtained product was cloned into the mammalian expression vector pEGFP-C1

(BD Biosciences Clontech). The mutant forms of *sipA* were PCR amplified from pEGFP-SipA and cloned in pEGFP-C1. Expression vectors with deletions in the F1 domain (pEGFP-ΔF1ΔABD) and in the F2 domain (pEGFP-ΔF2) were engineered by overlap extension PCR. The two DNA fragments needed for the construction of these *sipA* mutant forms were amplified by PCR, gel purified, and fused in one PCR. The full-length *sipA* and the mutant forms were expressed as a fusion to the C terminus of the enhanced GFP (EGFP). Construction of Myc-SipA was obtained by cloning the full-length *sipA* generated by PCR from pEGFP-SipA into pCMV-myc (Clontech). The full-length human NOD1 and dominant-negative versions of human NOD1 (hNOD1) and hNOD2 were PCR amplified from pUNO-hNOD1 and pUNO-hNOD2 (InvivoGen), respectively. hNOD1DN (amino acids [aa] 127 to 954) lacks the N-terminal caspase recruitment domain (CARD). hNOD2DN (aa 217 to 1041) lacks the two N-terminal CARDs. The obtained PCR products were cloned into a derivative of the mammalian expression vector pTracer-CMV2 (Invitrogen, Life Technologies). The derivative lacks the GFP gene and contains a 3×Flag tag at the C-terminal cloning site (42). The human *RIP2* gene was PCR amplified from cDNA prepared from HEK293 cells. The obtained PCR product was cloned into pTracer-CMV2, yielding pTracer-hRIP2 (aa 1 to 540). The dominant-negative form of hRIP2 (aa 1 to 434), lacking the C-terminal CARD, was PCR amplified from pTracer-hRIP2 and cloned into pCMV-HA (Clontech). The hemagglutinin (HA) tag is fused to the N terminus of hRIP2DN. The plasmid pDeNy-MyD88 expressing a dominant-negative human *MyD88* gene was purchased from InvivoGen. All constructs were verified by DNA sequencing.

Gentamicin protection assay. HEK293 and HeLa 57A cells were seeded in a 24-well tissue culture plate at approximately 50% confluence. At the time of infection, the cells had a confluence of approximately 100%. Overnight cultures of *S.* Typhimurium strains were diluted 1 in 50 and grown for 3 h at 37°C. HEK293 and HeLa 57A cells were infected with *S.* Typhimurium strains at approximately 10⁷ CFU/ml. The bacteria were incubated for 1 h at 37°C to allow invasion. The cells were washed three times with Dulbecco's phosphate-buffered saline (DPBS; pH 7.4) to remove extracellular bacteria, DMEM containing 10% FCS and gentamicin (0.1 mg/ml) was added, and the cells were incubated for 90 min at 37°C. The cells were washed in DPBS and lysed with 0.5 ml of 1% Triton X-100, and the lysates were transferred to a sterile Eppendorf tube. The wells were washed with 0.5 ml PBS and transferred to the Eppendorf tubes. Serial dilutions were plated on LB plates with the appropriate antibiotics to count the intracellular bacteria.

Transient transfection. HEK293 cells were grown in 24- or 48-well tissue culture plates in DMEM containing 10% FCS until 40% confluence was reached (~24 h). HEK293 cells were transiently transfected with a total of 250 ng of plasmid DNA, consisting of 25 ng of the reporter plasmid pNF-κB-luc, 25 ng of normalization vector pTK-LacZ, and 200 ng of either empty control vector, pUNO-hMyD88DN (InvivoGen), or pEGFP-SipA constructs. For the cotransfection experiments with pEGFP-SipA constructs and hNOD1DN-3×Flag, hNOD1DN-3×Flag, or HA-hRIP2DN, 100 ng of DNA for each plasmid was used. FuGene HD (Roche) was used as transfection reagent at a lipid-to-DNA ratio of 5 to 1. After 48 h of incubation, the cells were infected with the appropriate bacterial strains or the NOD1 ligand C12-iE-DAP, the NOD2 ligand MDP, or the TLR5 ligand flagellin (InvivoGen).

Luciferase assays. NF-κB activation was assessed using the NF-κB-luciferase reporter system. HeLa 57A cells stably transfected with an NF-κB-luciferase reporter construct and transiently transfected HEK293 cells were infected with the indicated *S.* Typhimurium strains (10⁷ CFU/ml) for 3 h, after which the cells were washed with DPBS and incubated at 37°C for an additional 2 h in the presence of DMEM containing 10% FCS. The cells were washed in DPBS and lysed in 0.1 ml of reporter lysis buffer (Promega). Firefly luciferase activity was measured with the luciferase assay system (Promega) using a plate reader. For normalization of the efficiency of transfection, luciferase values were adjusted to β-galactosidase values as determined with the β-galactosidase assay (Pro-

mega). Results were expressed as fold increase over the uninfected controls.

Protein expression analysis. HEK293 cells transfected with fusion proteins were lysed in lysis buffer (50 mM Tris-HCl, pH 7.6, 150 mM NaCl, 0.2% [vol/vol] NP-40, and 1 mM EDTA). An 0.01-mg amount of total protein was separated by SDS-polyacrylamide gel electrophoresis. Proteins were transferred to a polyvinylidene fluoride membrane (Millipore) in a semidry transfer process (Bio-Rad). The membranes were incubated in PBS containing 3% nonfat dry milk and 0.05% Tween 20 to block nonspecific binding. The membranes were incubated with polyclonal primary antibodies raised against tubulin (Cell Signaling Technology), mouse anti-Flag (Sigma), or mouse anti-HA (Covance). For GFP detection, a horseradish peroxidase (HRP)-conjugated anti-GFP antibody (Cell Signaling Technology) was used. HRP-conjugated anti-mouse IgG and HRP-conjugated anti-rabbit IgG (Promega) were used as the secondary antibodies for tubulin, Flag, and HA detection. Horseradish peroxidase activity was visualized by adding Immobilon Western chemiluminescent substrate (Millipore) to the membrane. Images were recorded and processed by a BioSpectrum imaging system (UVP).

Coimmunoprecipitation. HEK293 cells were transiently transfected for 48 h and lysed with lysis buffer (50 mM Tris-HCl, pH 7.6, 150 mM NaCl, 0.1% [vol/vol] NP-40, 1 mM EDTA, and protease inhibitors). Samples of the whole-cell lysate were collected for analysis by SDS-PAGE and immunoblotting. The whole-cell lysate was incubated for 2 h at 4°C with Dynal protein G beads (Invitrogen) coated with anti-Flag M2 antibody (Sigma). After 10 washes with the lysis buffer and 2 washes with 50 mM ammonium bicarbonate, samples of the immunoprecipitate were collected and subjected to SDS-PAGE and immunoblotting. The proteins of interest were detected with anti-Flag M2 antibody (Sigma), anti-Myc antibody (Cell Signaling), and anti-GFP antibody (Sigma).

Fluorescence microscopy. HEK293 cells were transfected with GFP-SipA and NOD1-Flag. After 48 h, the cells were washed and fixed with 3% paraformaldehyde. The cells were permeabilized with 0.1% saponin-10% goat serum (blocking reagent) in PBS for 30 minutes at room temperature. After blocking, cells were incubated with anti-Flag M2 antibody (1:1,000 dilution; Sigma) in 0.1% saponin and 10% goat serum in PBS for 1 h at room temperature. The cells were rinsed twice in 0.1% saponin in PBS and then twice in PBS and incubated (1 h) with Alexa Fluor 647 goat anti-mouse IgG (1:1,000 solution; Invitrogen). After the cells were rinsed twice in 0.1% saponin in PBS, twice in PBS, and once in H$_2$O, they were embedded in Fluorsave (Calbiochem) and analyzed with an LSM700 confocal microscope (Zeiss).

Animal experiments. Streptomycin (20 mg/mouse) (Sigma)-pretreated C57BL/6 mice (Jackson Laboratory) and NOD1/NOD2-deficient mice (generously provided by D. Portnoy) were mock infected with 0.1 ml of sterile LB broth or infected orally with 1×10^9 CFU (in 0.1 ml of LB broth) of an S. Typhimurium *sopABDE2* mutant (ZA20) or a *sipA sopABDE2* mutant (ZA21) carrying the plasmid pHP45Ω to confer streptomycin resistance. At 48 h after infection, mice were sacrificed, and samples of the cecum were snap-frozen in liquid nitrogen for isolation of mRNA.

Histopathology. Formalin-fixed, hematoxylin- and eosin-stained cecal tissue sections were blinded for evaluation by a veterinary pathologist. The following pathological changes were scored: (i) neutrophil infiltration, (ii) infiltration by mononuclear cells, (iii) submucosal edema, (iv) epithelial damage, and (v) inflammatory exudate. The pathological changes were scored on a scale from 0 to 4 as follows: 0, no changes; 1, detectable; 2, mild; 3, moderate; 4, severe. Images were taken using an Olympus BX41 microscope.

Real-time PCR. Samples of the cecum were collected, immediately snap-frozen in liquid nitrogen, and stored at −80°C. RNA was extracted using TriReagent (Molecular Research) according to the instructions of the manufacturer. Reverse transcription was performed on 1 μg of DNase-treated RNA with TaqMan reverse transcription reagent (Applied Biosystems). For each real-time reaction, 4 μl of cDNA was used. Real

time transcription-PCR (RT-PCR) was performed using Sybr green (Applied Biosystems) and an ABI 7900 RT-PCR machine (Applied Biosystems). The fold change in mRNA levels was determined using the comparative threshold cycle (C_T) method (Applied Biosystems). Target gene transcription was normalized to the levels of glyceraldehyde-3-phosphate dehydrogenase (GAPDH) mRNA.

Statistical analysis. A paired Student t test was used to confirm statistical significance in the tissue culture experiments. To determine statistical significance of the relative mRNA transcription between treatment groups in the animal experiments, an unpaired Student t test was used. To determine the statistically significant differences in the total histopathology scores, a Mann-Whitney U test was used. A two-tailed P value of <0.05 was taken to be significant.

SUPPLEMENTAL MATERIAL

Supplemental material for this article may be found at http://mbio.asm.org/lookup/suppl/doi:10.1128/mBio.00266-11/-/DCSupplemental.

Figure S1, PDF file, 0.1 MB.
Figure S2, PDF file, 0.2 MB.
Figure S3, PDF file, 0.7 MB.
Figure S4, PDF file, 2.8 MB.

REFERENCES

1. **Tsolis RM, Adams LG, Ficht TA, Bäumler AJ.** 1999. Contribution of *Salmonella typhimurium* virulence factors to diarrheal disease in calves. Infect. Immun. **67**:4879–4885.
2. **Winter SE, et al.** 2010. Gut inflammation provides a respiratory electron acceptor for salmonella. Nature **467**:426–429.
3. **Lawley TD, et al.** 2008. Host transmission of *Salmonella enterica* serovar Typhimurium is controlled by virulence factors and indigenous intestinal microbiota. Infect. Immun. **76**:403–416.
4. **Barthel M, et al.** 2003. Pretreatment of mice with streptomycin provides a *Salmonella enterica* serovar Typhimurium colitis model that allows analysis of both pathogen and host. Infect. Immun. **71**:2839–2858.
5. **Fu Y, Galán JE.** 1998. The *Salmonella typhimurium* tyrosine phosphatase SptP is translocated into host cells and disrupts the actin cytoskeleton. Mol. Microbiol. **27**:359–368.
6. **Zhou D, Mooseker MS, Galán JE.** 1999. An invasion-associated salmonella protein modulates the actin-bundling activity of plastin. Proc. Natl. Acad. Sci. U. S. A. **96**:10176–10181.
7. **Friebel A, et al.** 2001. SopE and SopE2 from *Salmonella typhimurium* activate different sets of RhoGTPases of the host cell. J. Biol. Chem. **276**:34035–34040.
8. **Hong KH, Miller VL.** 1998. Identification of a novel salmonella invasion locus homologous to Shigella ipgDE. J. Bacteriol. **180**:1793–1802.
9. **Jepson MA, Kenny B, Leard AD.** 2001. Role of sipA in the early stages of *Salmonella typhimurium* entry into epithelial cells. Cell. Microbiol. **3**:417–426.
10. **Raffatellu M, et al.** 2005. SipA, SopA, SopB, SopD, and SopE2 contribute to *Salmonella enterica* serotype Typhimurium invasion of epithelial cells. Infect. Immun. **73**:146–154.
11. **Zhou D, Mooseker MS, Galán JE.** 1999. Role of the *S. typhimurium* actin-binding protein SipA in bacterial internalization. Science **283**:2092–2095.
12. **Zhang S, et al.** 2002. The *Salmonella enterica* serotype Typhimurium effector proteins SipA, SopA, SopB, SopD, and SopE2 act in concert to induce diarrhea in calves. Infect. Immun. **70**:3843–3855.
13. **Hobbie S, Chen LM, Davis RJ, Galán JE.** 1997. Involvement of mitogen-activated protein kinase pathways in the nuclear responses and cytokine production induced by *Salmonella typhimurium* in cultured intestinal epithelial cells. J. Immunol. **159**:5550–5559.
14. **Hoffmann C, et al.** 2010. In macrophages, caspase-1 activation by SopE

and the type III secretion system-1 of *S. typhimurium* can proceed in the absence of flagellin. PLoS One **5**:e12477.

15. **Miao EA, et al.** 2006. Cytoplasmic flagellin activates caspase-1 and secretion of interleukin 1beta via Ipaf. Nat. Immunol. **7**:569–575.

16. **Miao EA, et al.** 2010. Innate immune detection of the type III secretion apparatus through the NLRC4 inflammasome. Proc. Natl. Acad. Sci. U. S. A. **107**:3076–3080.

17. **Hapfelmeier S, et al.** 2005. The salmonella pathogenicity island (SPI)-2 and SPI-1 type III secretion systems allow *Salmonella serovar typhimurium* to trigger colitis via MyD88-dependent and MyD88-independent mechanisms. J. Immunol. **174**:1675–1685.

18. **Adachi O, et al.** 1998. Targeted disruption of the MyD88 gene results in loss of IL-1- and IL-18-mediated function. Immunity **9**:143–150.

19. **Muzio M, Ni J, Feng P, Dixit VM.** 1997. IRAK (Pelle) family member IRAK-2 and MyD88 as proximal mediators of IL-1 signaling. Science **278**:1612–1615.

20. **Wesche H, Henzel WJ, Shillinglaw W, Li S, Cao Z.** 1997. MyD88: an adapter that recruits IRAK to the IL-1 receptor complex. Immunity **7**:837–847.

21. **Figueiredo JF, et al.** 2009. *Salmonella enterica Typhimurium* SipA induces CXC-chemokine expression through p38MAPK and JUN pathways. Microbes Infect. **11**:302–310.

22. **Isberg RR, Voorhis DL, Falkow S.** 1987. Identification of invasin: a protein that allows enteric bacteria to penetrate cultured mammalian cells. Cell **50**:769–778.

23. **Lu W, et al.** 2006. Cutting edge: enhanced pulmonary clearance of *Pseudomonas aeruginosa* by Muc1 knockout mice. J. Immunol. **176**:3890–3894.

24. **Smith MF, Jr, et al.** 2003. Toll-like receptor (TLR) 2 and TLR5, but not TLR4, are required for *Helicobacter pylori*-induced NF-kappa B activation and chemokine expression by epithelial cells. J. Biol. Chem. **278**:32552–32560.

25. **Schlumberger MC, et al.** 2007. Two newly identified SipA domains (F1, F2) steer effector protein localization and contribute to salmonella host cell manipulation. Mol. Microbiol. **65**:741–760.

26. **Geddes K, et al.** 2010. Nod1 and Nod2 regulation of inflammation in the salmonella colitis model. Infect. Immun. **78**:5107–5115.

27. **Le Bourhis L, et al.** 2009. Role of Nod1 in mucosal dendritic cells during salmonella pathogenicity island 1-independent *Salmonella enterica* serovar Typhimurium infection. Infect. Immun. **77**:4480–4486.

28. **Girardin SE, et al.** 2001. CARD4/Nod1 mediates NF-kappaB and JNK activation by invasive *Shigella flexneri*. EMBO Rep. **2**:736–742.

29. **Inohara N, et al.** 2000. An induced proximity model for NF-kappa B activation in the Nod1/RICK and RIP signaling pathways. J. Biol. Chem. **275**:27823–27831.

30. **Argast GM, Fausto N, Campbell JS.** 2005. Inhibition of RIP2/RIck/CARDIAK activity by pyridinyl imidazole inhibitors of p38 MAPK. Mol. Cell. Biochem. **268**:129–140.

31. **Bruno VM, et al.** 2009. *Salmonella typhimurium* type III secretion effectors stimulate innate immune responses in cultured epithelial cells. PLoS Pathog. **5**:e1000538.

32. **Müller AJ, et al.** 2009. The *S. typhimurium* effector SopE induces caspase-1 activation in stromal cells to initiate gut inflammation. Cell Host Microbe **6**:125–136.

33. **Lee CA, et al.** 2000. A secreted salmonella protein induces a proinflammatory response in epithelial cells, which promotes neutrophil migration. Proc. Natl. Acad. Sci. U. S. A. **97**:12283–12288.

34. **McCormick BA, Colgan SP, Delp-Archer C, Miller SI, Madara JL.** 1993. *Salmonella typhimurium* attachment to human intestinal epithelial monolayers: transcellular signalling to subepithelial neutrophils. J. Cell Biol. **123**:895–907.

35. **Silva M, Song C, Nadeau WJ, Matthews JB, McCormick BA.** 2004. *Salmonella typhimurium* SipA-induced neutrophil transepithelial migration: involvement of a PKC-alpha-dependent signal transduction pathway. Am. J. Physiol. Gastrointest. Liver Physiol. **286**:G1024–G1031.

36. **Wall DM, et al.** 2007. Identification of the *Salmonella enterica serotype typhimurium* SipA domain responsible for inducing neutrophil recruitment across the intestinal epithelium. Cell. Microbiol. **9**:2299–2313.

37. **Hapfelmeier S, et al.** 2004. Role of the salmonella pathogenicity island 1 effector proteins SipA, SopB, SopE, and SopE2 in *Salmonella enterica* subspecies 1 serovar Typhimurium colitis in streptomycin-pretreated mice. Infect. Immun. **72**:795–809.

38. **Stojiljkovic I, Bäumler AJ, Heffron F.** 1995. Ethanolamine utilization in *Salmonella typhimurium*: nucleotide sequence, protein expression and mutational analysis of the cchA cchB eutE eutJ eutG eutH gene cluster. J. Bacteriol. **177**:1357–1366.

39. **Raffatellu M, et al.** 2009. Lipocalin-2 resistance confers an advantage to *Salmonella enterica serotype Typhimurium* for growth and survival in the inflamed intestine. Cell Host Microbe **5**:476–486.

40. **Wang RF, Kushner SR.** 1991. Construction of versatile low-copy-number vectors for cloning, sequencing and gene expression in *Escherichia coli*. Gene **100**:195–199.

41. **Rodriguez MS, Thompson J, Hay RT, Dargemont C.** 1999. Nuclear retention of IkappaBalpha protects it from signal-induced degradation and inhibits nuclear factor kappaB transcriptional activation. J. Biol. Chem. **274**:9108–9115.

42. **Keestra AM, de Zoete MR, Bouwman LI, van Putten JP.** 2010. Chicken TLR21 is an innate CpG DNA receptor distinct from mammalian TLR9. J. Immunol. **185**:460–467.